A COMPLETE SAMPLE OF WHITE DWARFS, HOT SUBDWARFS, AND QUASARS

Thesis by

Richard Frederick Green

In Partial Fulfillment of the Requirements

for the Degree of

Doctor of Philosophy

California Institute of Technology

Pasadena, California

1977

(Submitted May 23, 1977)

To my wife Joanie
whose affection, enthusiasm and encouragement
have been a sustaining force

and

To my parents
who reared me to cherish the values implicit
in education and scholarship

ACKNOWLEDGMENTS

The most pleasant task in the preparation of this thesis is the acknowledgment of those who have influenced, guided, and helped me as a graduate student:

Dr. Maarten Schmidt, whose patience, support, and participation have made this project possible. His rigorous, critical thinking, combined with his fairness, practicality, and good humor have made his many hours of thoughtful instruction and discussion inestimably valuable;

Dr. Jesse Greenstein, who has been so generous with his time and energy in communicating his encyclopedic knowledge and active scientific curiosity about the faint blue stars;

Dr. Allan Sandage, who has cheerfully provided continuing encouragement, insightful discussions, and data prior to publication;

Drs. James Gunn, J. B. Oke, and W. L. W. Sargent, who have always made time to be helpful, both in giving scientific advice and by taking responsibility for the health and well-being of the Palomar telescopes and instruments upon which I relied;

The late Mr. Dennis Palm, Mr. Chip Williams, and Mr. Eugene Hancock, who have with skill and friendship handled the telescopes on clear nights and the astronomer on

cloudy nights;

Messrs. Martin Olsiewski, Bud Smith, Larry Blakeé, and Bob Cadman, who have kept the observatory electronics working through a combination of persistence and magic;

Mr. Michael Morrill of Jet Propulsion Laboratory, who has been a friend and valued collaborator in the scanning and reduction of the survey films;

The past and present denizens of Robinson, who have provided friendship, help, and intellectual enrichment through these years. A necessarily incomplete list includes Helen Z. K. Fridenberg, Lilo Hauck, Paul Hickson, John Hoessel, John Huchra, John Kormendy, Charles Kowal, Doug Richstone, Anneila Sargent, Ed Turner, Barry Turnrose, Steve Willner, and especially Ted Williams and Doug Rabin, my collaborators in certain unpublished works of drama;

Mrs. Helen Holloway, who has constantly demonstrated her affection and concern for Caltech and its students, from the day I arrived through the preparation and typing of this manuscript;

The National Science Foundation and the California Institute of Technology, both of which have provided financial support;

Joan Auerbach Green, to whom this thesis is dedicated, has spent many hours assisting in the preparation of

observing and film scanning programs, and of this manuscript. I am grateful for her willing expenditure of time and effort, and even more for her companionship and understanding during the last four years.

ABSTRACT

An analysis is made of a complete sample of hot white dwarfs, identified spectroscopically from candidates selected for ultraviolet excess without regard to proper motion. The luminosity function and local space density of hot white dwarfs are derived, giving 1.43 ± .28 per 1000 cubic parsecs for $M_V < 12.75$. A model of the local rate of star formation is constructed, which, when combined with white dwarf cooling theory, satisfactorily reproduces the observed luminosity function. The predicted densities at fainter absolute magnitudes also agree with the observations although uncertainties in the data do not allow a determination of the change in star formation rate with time. The model predicts a range of scale heights for hot white dwarfs of 220 to 270 pc, and a total local density of degenerate stars of at least 20 per 1000 cubic parsecs. The assumption of a single population of DA white dwarfs with identical composition is not adequate to explain the observed color-color diagram.

A breakdown by spectral type of the entire complete sample of ultraviolet excess objects shows that the hot white dwarfs comprise 70% of the faint blue stars to a mean limiting magnitude of B = 15.7. The mean local density of subdwarf B stars is found to be $(1.4 \pm .5) \times 10^{-9}$ pc^{-3},

representing only .0005 of the number of stars on the halo horizontal branch, and thereby explaining their near absence in globular clusters. The mean local density of subdwarf O stars of $(3.4 \pm 1.2) \times 10^{-9}$ pc^{-3} makes unlikely the possibility that these stars have any direct evolutionary connection with the observed Population I hot white dwarfs or planetary nebulae. The local space density of quasars is derived on the assumption of cosmological redshifts, and provides no contradiction to the hypothesis of a smooth transition between the phenomena of Seyfert galaxy nuclei and quasars. Both the space and surface densities are consistent with the luminosity function and density evolution laws found by Schmidt (1972); the statistical uncertainties in the present case are too great to determine the choice of density laws.

The validity of these statistical studies depends upon the objective selection of a sample within well-defined limits of magnitude and color. To that end, computer programs have been developed for use in collecting and processing data from a PDS scanning microdensitometer. The goal is to obtain fast and simple algorithms for handling an entire astronomical photograph with one-pass digitization. This capability is realized by a real-time detection scheme that provides a data compression of a factor of 100, and a

processing program that produces a catalogue of magnitudes, colors, and positions for up to 90,000 multicolor stellar images.

TABLE OF CONTENTS

INTRODUCTION

This thesis consists of three independent papers related to the topic of isolating and analyzing a complete sample of stellar objects selected on the basis of ultraviolet excess. Some redundancy and discontinuity between chapters were therefore unavoidable, and the reader's indulgence is requested. It is also regretted that the catalogue of the data that form the basis for this investigation was not tabulated in time for inclusion in the thesis; this material will be available in the published version.

A four-stage observational program was undertaken to generate the data under discussion. Two-color survey films were taken on the Palomar 18-inch Schmidt telescope covering 10,000 square degrees of the sky at high galactic latitude. Those stellar objects selected from the films for ultraviolet excess were observed and classified spectroscopically, and all white dwarfs were reobserved photoelectrically in the Strömgren system. At the same time, a broad-band photoelectric sequence was established for each field to transform the photographic magnitudes. These papers represent the results derived from the first 15% of the total survey. The first chapter reports on the white dwarf study and its interpretation in terms of a star formation model;

the second chapter treats the other spectral types discovered. The final chapter will be published with Michael Morrill of the Image Processing Laboratory at Jet Propulsion Laboratory as co-author; it describes the technique for computer analysis of the survey films.

CHAPTER 1

THE LUMINOSITY FUNCTION OF HOT WHITE DWARFS: OBSERVATIONS OF A COMPLETE SAMPLE AND PREDICTIONS OF A MODEL OF THE LOCAL RATE OF STAR FORMATION

I. INTRODUCTION

The luminosity function of white dwarfs contains information valuable for determining the evolution of white dwarfs through cooling processes and the rate of formation of their progenitors on the upper main sequence. Luyten (1958) first produced preliminary estimates of the total space density of white dwarfs from counts of proper motion objects. Weidemann (1967) made a fundamental synthesis of spectroscopic data from Eggen and Greenstein (1965) and Sandage and Luyten (1967) as well as proper motion data from Luyten (1963-66). He derived a luminosity function for comparison with white dwarf cooling theories of Mestel (1952) and Mestel and Ruderman (1967), using the theory to predict the total local density of white dwarfs. More recently, Sion and Liebert (1977) have made a redetermination from all available spectroscopic and photometric data on white dwarfs. Their comparison with detailed evolutionary models of Lamb and Van Horn (1975) shows generally good agreement.

An acknowledged difficulty in these analyses has been isolating a statistically valid sample from heterogeneous observational material. The present paper reports on observations that were made specifically to obtain a complete sample based on ultraviolet excess. Over 1/3 of the

faintest stars were ultimately rejected to create a final complete list of 81 white dwarfs, on which this analysis is based. Only 10 of these were previously known from proper motion catalogues, indicating that the present survey covers a more substantial volume, especially for the hottest stars.

There are further complications in comparing the observed luminosity function with theoretical cooling curves. One must consider the rate of input of new white dwarfs into the cooling sequence, that is, the rate of formation of their upper main sequence progenitors, which may be a changing function of time. The local space density of white dwarfs may also be diluted by dynamical expansion of the white dwarf disk layer. To study these effects, a model of local star formation is constructed, following Schmidt (1959, 1963). The rate of star formation, dynamical evolution of mean distances perpendicular to the galactic plane, and the white dwarf cooling curve from Lamb and Van Horn (1975) are then combined to predict the white dwarf luminosity function.

The observations and white dwarf absolute magnitude calibration are discussed in §II, then the observed luminosity function and space density are presented in §III. The construction of the star formation and dynamical evolution models is described in §IV, some remarks on the astrophysical implications of the white dwarf color-color diagram are

found in §V, and a brief summary comprises §VI.

II. THE OBSERVATIONAL DATA AND ABSOLUTE MAGNITUDE DETERMINATION

The basis for this statistical study is a complete sample of hot white dwarfs selected solely on the basis of ultraviolet excess without regard to proper motion. The objects were chosen from 26 two-color films covering 1434 square degrees above $|b| = 37°$ taken on the Palomar 18-inch Schmidt telescope (Green 1976). Initial visual inspection was later followed by computer processing of most films (Green 1977), so the selection process should be relatively free of subjective error. Out of the 20,000 stars on each film brighter than a limit near blue magnitude 16.5, about 10 were isolated for showing the strongest ultraviolet excess. These objects were then observed on the Palomar 1.5 meter telescope with the Cassegrain image-tube spectrograph at an inverse dispersion of 280 Å mm^{-1} for classification. The faintest ones were observed by Dr. Maarten Schmidt on the Palomar 5-meter telescope with the Cassegrain image-tube spectrograph and, more recently, the SIT spectrograph, at an inverse dispersion of 190 Å mm^{-1}.

Any star with a spectrum containing broad hydrogen Balmer lines or broad helium lines was classified as a white dwarf. Some objects showing no strong spectral features were reobserved photometrically in the Strömgren

system, as discussed below, or on the 5-meter telescope by Drs. Schmidt or J. L. Greenstein with the multi-channel spectrophotometer, after which classifications were made based on the energy distributions. The difficulty in deciding whether a weak-lined star is degenerate without any knowledge of its kinematics is epitomized in the case of PG 2337+12 (Green, Greenstein and Boksenberg 1976), which was originally classified as a white dwarf but turned out to be a cataclysmic variable. Those stars showing the H and K lines of ionized calcium were not included in the sample. The survey was intended to have a color limit of $U-B < -0.4$; it can be seen in the color-color diagrams of Greenstein (1966) and Sandage and Luyten (1969) that a limit of $U-B = -0.5$ cleanly discriminates against the subdwarf G stars and the cooler white dwarfs. The difficulty in distinguishing between the latter two types of objects by either colorimetric or spectroscopic criteria led to the decision to exclude stars with calcium H and K from the final list. Although the importance of extending the luminosity function to cooler degenerates was recognized, the present sample is necessarily incomplete in this U-B color range, and could not have contributed an accurate value.

The next step in the observational procedure was to measure in the Strömgren 4-color system each star classified as a white dwarf. Graham (1972) demonstrated the effectiveness of this color system in yielding direct

information on the physical properties of white dwarfs. In particular, the color index b-y is a line-free measure of the continuum in DA stars and was shown to be strongly correlated with the absolute magnitudes derived from trigonometric parallaxes, with a dispersion of only $0^m.27$. Graham found that the index $m_1 = (v-b) - (b-y)$ is a direct determination of the hydrogen line strength, from its correlation with the equivalent width of Hγ. Another major result of his work is the remarkably narrow sequence defined by the DA white dwarfs in the u-b, b-y diagram, implying a very low scatter in the value of log g, the surface gravity.

Graham also cautioned that uvby is a filter-defined system, so that special care must be taken in the transformations. The set of filters used in this investigation is described in Table 1; measurement on a scanning spectrometer shows them to be very similar to the filter set described by Crawford and Barnes (1970). To avoid uncertain coincidence corrections for the photometer on the Palomar 1.5-meter telescope, standard stars must be chosen fainter than 8th magnitude; consequently, primary system standards could not be used. In order to take into account specifically the effects of the broadened lines in white dwarfs, a list of secondary standards was compiled from Graham's (1972) uvby photometry of white dwarfs, with some redder objects added from his lists of Feige stars (1970). The average residuals of the transformations were $0^m.05$ in V, $0^m.02$ in b-y, and

TABLE 1

STROMGREN FILTERS

BAND	CENTRAL WAVELENGTH (ANGSTROMS)	FULL WIDTH HALF MAXIMUM (ANGSTROMS)	TYPE
u	3425	370	Schott Glass 8mm UG11 + 1mm WG3
v	4122	212	Interference
b	4691	217	Interference
y	5500	190	Interference

$0^m.05$ in u-b, defining the accuracy for a single measurement, with the exception of objects fainter than 16th magnitude, for which systematic errors in centering become important. Since every star was measured in both channels of the dual channel photometer, each of which was reduced separately, the quoted uncertainty is reduced by a factor of $\sqrt{2}$, and many objects were measured on 2 nights, further increasing the accuracy. Since Strömgren photometry had not been done previously on Palomar, standard mean values of the extinction were not available. The extinction was therefore derived each night in a simultaneous solution for the transformation constants (Huchra 1976). The second-order extinction terms were all assumed to be 0.

The measurement of b-y for each white dwarf in the sample allows the computation of M_V from a linear regression on Graham's (1972) data

$$M_V = 7.56\ (b-y) + 11.50, \text{ with } \sigma = 0^m.27.$$

This determination includes all spectral types; the presence of He I λ4713 absorption in the b filter does not seem to introduce a significant systematic bias for the DB stars, in face of the larger calibration uncertainties. In cases where multichannel spectrophotometry was available, Greenstein's (1977) monochromatic color indices were also used to derive the absolute magnitude. For stars measured in both systems, the agreement was consistent with Greenstein's quoted uncertainty of $0^m.6$, and the value derived from the

Strömgren colors was used for uniformity. Likewise, M_V was determined for those stars with broad-band colors by using the calibration of B-V by Sion and Liebert (1977). Again, comparison of absolute magnitudes obtained from the two calibrations was consistent with the dispersion of their fit of $0^m.24$.

As described above, recent computer processing has expanded the list of candidates found by visual inspection, so that several white dwarfs have been discovered spectroscopically for which photoelectric photometry has not been possible. For two of those DA stars, sufficiently high quality SIT spectra were obtained that the equivalent width of Hγ could be measured with some accuracy. Graham's (1972) empirical relationship between W(Hγ) (as expressed by m_1) and b-y is very tight, and shows a maximum at W(Hγ) $\sim$ 40 Å. Both the photographic U-B colors and the energy distributions through the slit show that the 2 objects lie on the blue side of the relation, so that b-y and M_V were estimated for them, with the greater uncertainty noted. The effects of interstellar reddening and absorption were neglected in all cases, because of the relatively small distances of the white dwarfs and their high galactic latitude.

The photoelectric magnitudes were measured in visual light and the absolute magnitudes were also derived on the V scale. The objects were selected, however, from films that were magnitude limited in B, so it is necessary to

know B-V for the statistical study. It is apparent that b-y would transform directly to B-V if it were not for the presence of strong Hγ, but m_1 is an indicator of the strength of Hγ. A bilinear transformation was therefore derived from the photometry of Graham (1972) and Eggen and Greenstein (1965)

$$B-V = 1.57\ (b-y) + 0.67\ m_1 - 0.12$$

with a dispersion of less than $0^m.02$. Types DB and DC were included in this calibration; although there is a small systematic error in the transformation for the DB's, the B magnitudes derived in this way are still much more accurate than photographic magnitudes determined to $0^m.2$.

III. THE LOCAL SPACE DENSITY AND LUMINOSITY FUNCTION OF WHITE DWARFS

The crucial quantity in the definition of a complete sample for statistical study is the limiting magnitude. The V/V_m method, as discussed by Schmidt (1968), is a powerful test of the completeness of a sample. If V is the volume defined by the observed radial distance to an object and V_m the volume defined by the maximum distance at which the object would still appear in the magnitude limited sample, then the average of V/V_m would be 0.5, with an uncertainty of $(12n)^{-\frac{1}{2}}$ assuming a uniform distribution for n objects. For a single photograph, the procedure would be to pick a first estimate of the completeness limit near the limiting

magnitude of the film and compute $\langle V/V_m \rangle$ from the measured apparent magnitudes. If the value is less than 0.5, the completeness limit is made brighter until $\langle V/V_m \rangle = 0.5$ to within the errors.

The situation is in reality more complicated for two reasons. First, variations in transparency, film sensitivity, and telescope focus produce a different limiting magnitude for each film in the survey. Second, the assumption of uniform space density will not be valid for a population of white dwarfs with a density gradient perpendicular to the plane of the Galaxy.

The number of white dwarfs on any given film is too small to use the V/V_m test to determine the limit for that film. The initial guess for the completeness limit of each film was made by a visual count of the total number of stars within a .54 square degree area in the center of the film. This technique allows a determination of the average number of stars per square degree on the film to an accuracy of better than 10%. The observed surface densities were then compared to those derived by van Rhijn (1929) for the same galactic latitude to get the limiting photographic magnitude accurate to $0^m.1$. Arp's (1965) relationship $B = m_{pg} + 0.1 + 0.1\ (m_{pg} - 14.0)$ was used to transform to the B system.

Even a complete sample, if selected from a population with a non-uniform space distribution such as a thin disk system, will produce $\langle V/V_m \rangle < 0.5$. Schmidt (1968) explained that use of the density-weighted volume, in this case $dV' = dV \; D(z)$ where $D(z)$ is the normalized density distribution perpendicular to the plane, will return the value of $\langle V'/V_m' \rangle$ to 0.5 for a complete sample.

The V/V_m test was applied to the present sample of white dwarfs by first using the initial estimates of the limiting magnitudes derived from the surface densities. The result was $0.32 \pm .03$, far from completeness. Next, the effect of the non-uniform space distribution was tested by assuming a run of densities of the form $D(z) = e^{-z/z_o}$ with a scale height of 150 pc. This density weighting increased $\langle V/V_m \rangle$ by only .05. The implication is that the sample of white dwarfs initially selected was not complete down to the very limit of each film, and that a space distribution had to be assumed to determine the actual completeness limits from $\langle V'/V_m' \rangle$. Scale heights as a function of absolute magnitude with a range of 245 to 270 pc were adopted from a detailed model, as discussed in the next section. All the magnitude limits were then made brighter by an equal amount and the test repeated until the sample was considered sufficiently complete for a valid statistical study. With final limiting magnitudes $0\overset{m}{.}8$ brighter than those originally determined from the surface densities, over 1/3 of the

faintest stars had been eliminated from the sample to produce $\langle V'/V'_m \rangle = 0.46 \pm .03$.

The resulting sample was then used to derive the local luminosity function for hot white dwarfs by means of a method discussed by Schmidt (1975). For each star in a magnitude limited sample, its contribution to the local space density is $1/V'_m$. Combining the values for all stars in the sample gives a series of weighted delta functions distributed in absolute magnitude, the envelope of which defines the luminosity function. The difficulty again arises that each film has a different completeness limit. The problem can be circumvented by deriving a maximum volume for the entire survey as a function of absolute magnitude. In other words, a white dwarf of given absolute magnitude would define a maximum sampled volume for each field, so its contribution to the luminosity function is 1 divided by the union of all the individual maximum volumes. In the case of overlapped adjacent fields, the area of overlap was assigned to the field with the fainter limiting magnitude, and subtracted from the other. The density weighting was determined by computing z_m from the galactic latitude and magnitude limit for each field, then using the scale height from the model. The derived luminosity function is not sensitive to this choice of scale heights; a factor of 2 change in scale height affects the result by 15%.

For presentation purposes, the objects were grouped

into ½-magnitude bins. The results are presented in Table 2 and Figure 1. The quoted uncertainties are simply statistical, and do not include the effects of errors in photometry or absolute magnitude calibration. The total number of white dwarfs per 1000 cubic parsecs is 1.43 ± .28 for M_V < 12.75, and with greater uncertainty 2.42 ± .57 for M_V < 13.25.

This determination of the luminosity function and space density of hot white dwarfs is the first to be based on a complete sample of spectroscopically identified white dwarfs. Luyten (1958) derived an empirical luminosity function from the fractional contribution of white dwarfs to the general luminosity function of proper motion stars. Weidemann (1967) constructed luminosity functions from two sets of published data available to him: a large list of objects classified by Luyten (1963-1966) as white dwarfs on the basis of color and proper motion, and the list of spectroscopically identified white dwarfs from Eggen and Greenstein (1965). The inherent difficulties in using those lists are the lack of spectroscopic identifications in the former and the diversity of selection criteria of the latter. To find limits of relative completeness in apparent magnitude, Weidemann assumed a uniform density distribution of white dwarfs. The V/V_m test applied to the present sample shows that assumption beginning to break down at a mean B magnitude limit of 15.7; Luyten's material reaches to 21st

TABLE 2

LUMINOSITY FUNCTION OF WHITE DWARFS

M_V	10.0	10.5	11.0	11.5	12.0	12.5	13.0
$\phi(M_V)$ $(10^{-3}pc^{-3}(\frac{1}{2}mag)^{-1})$	.020	0.13	0.19	0.22	0.34	0.52	0.99
$\pm$	.007	0.03	0.04	0.07	0.13	0.23	0.50

magnitude. Weidemann also did not take into account the area of the sky covered by Eggen and Greenstein's lists. Sion and Liebert (1977) used Weidemann's technique on their larger list of spectroscopically identified white dwarfs, which was subject to the same difficulties. The relative shapes of the luminosity functions so derived appear to be representative. The absolute value of the local space density, however, cannot be accurately determined by this method, as witnessed by the factor of 5 spread in Weidemann's values. For comparison purposes, Weidemann's estimates were transformed to the number density for $M_V < 12.75$, and they bracket the results of the present investigation.

Eggen (1968) has done extensive photoelectric photometry of proper motion stars, from which he estimated the total number of hot white dwarfs in the first 180 fields of the Lowell Proper Motion Survey (contained in Giclas et al. 1971). His defined U-B color limit for this group was approximately the same as that of the present sample. By considering both the completeness limit of his material and the area of coverage, he obtained a lower limit to the mean density of 1 per 1000 cubic parsecs. His use of Luyten's (1965) fractional distribution of hot white dwarfs among proper motion stars produced a value of 2 per 1000 cubic parsecs. These estimates are in reasonable agreement with the densities derived in this paper.

The luminosity function of white dwarfs contains information about the cooling rate of degenerate stars and about the rate of star formation of the progenitors. The shape of the cooling curve can be compared directly with the luminosity function only if one assumes a constant rate of input of hot white dwarfs; that is, a constant rate of star formation, and that there is no dilution of the space density by a gradual increase in scale height brought about by dynamical interactions. To relax these assumptions, a more detailed model of star formation and dynamical evolution must be computed.

IV. MODELS OF THE RATE OF STAR FORMATION AND WHITE DWARF LUMINOSITY FUNCTION

To determine the rate of input to the white dwarf cooling sequence, the rate of star formation of the progenitors must be known as a function of time. The formulation of the problem as developed by Schmidt (1959, 1963) was used in the present investigation. The rate of star formation is derived for the solar neighborhood, assuming it is a smooth function of time for stars of a given mass and that the lifetimes and masses of stars of a given luminosity are not a function of the time of formation; that is, enrichment of

composition is neglected. It is observed that the mean distance perpendicular to the plane of the galaxy increases with later spectral type. Since Oort (1958) has shown that the z-distance of galactic clusters increases for later main sequence turn-off, the further assumption is made that the z-width of a population distribution increases with increasing age. To compensate for this effect, the rates are computed for a cylinder of one square parsec cross-sectional area perpendicular to the galactic plane at the sun.

We shall consider the problem of star formation for the adopted age of the Galaxy as a unit time interval of 1.5×10^{10} years, with t = 1 being the present, during which the amount of gas available for star formation was depleted by a factor of 5. Let $N(M_V,t)$ be the number of stars per square parsec formed up to time t in the magnitude interval $M_V - \frac{1}{2}$ to $M_V + \frac{1}{2}$, and $\Psi(M_V)$ be the present rate of formation of stars of brightness M_V, per square parsec. Further, define

$$g(t) = \mathfrak{M}_g(t)/\mathfrak{M}_g(1) \qquad (1)$$

the surface density of gas available for star formation in units of the present density, with $g(1) = 1$, and $g(0) = 5$. The rate of star formation is then expressed as

$$\frac{dN(M_V,t)}{dt} = \psi(M_V)\ [g(t)]^n \qquad (2)$$

where the rate is assumed proportional to some power of the gas density. Schmidt's (1963) derivation included a mass-dependent term in the exponent to account for the observed metal abundances in late G-type dwarfs. The white dwarf luminosity function is very insensitive to the brightest main sequence stars, so that term was omitted here.

If $\Phi(M_V)$ is defined as the main sequence luminosity function per square parsec presently observed, and $T(M_V)$ the main sequence lifetime for stars of absolute magnitude M_V, then from equation (2)

$$\Phi(M_V) = N(M_V,1) - N[M_V,1-T(M_V)] = \Psi(M_V) \int_{1-T(M_V)}^{1} [g(t)]^n \, dt \quad (3)$$

The main sequence luminosity function consists of all stars formed less than one main sequence lifetime ago. For massive stars, $T(M_V) << 1.5\times10^{10}$ years, and

$$\Phi(M_V) \approx \Psi(M_V)\ T(M_V) \quad (4)$$

Schmidt (1959) derived analytical approximations for g(t) by solving for the depletion of the interstellar gas by star formation

$$n = 1 \qquad g(t) = 5^{1-t} \quad (5a)$$

$$n = 2 \qquad g(t) = 5/(1+4t) \quad (5b)$$

The above is a brief restatement of the relevant aspects of the problem as formulated by Schmidt. The fundamental data used in the computations are presented in Table 3. The second column lists the masses corresponding to the absolute magnitudes, as given by Schmidt (1963). The third column contains the luminosity function of McCuskey (1966), corrected and smoothed to represent the main sequence. Giant stars contribute significantly to his counts only at absolute magnitudes 0 and +1. The values of the composite luminosity function at these magnitudes were replaced by the corresponding entries of a luminosity function constructed from densities given for main sequence stars alone. The fourth column lists the values of twice the mean z-distance for the spectral type, as given by Blaauw (1965). The resulting surface density, Φ', follows. One further correction must be applied. McCuskey's luminosity function was derived from counts based on objective prism plates, from which stars were assigned absolute magnitudes based on their spectral types. Evolutionary tracks by Iben (1965, 1966a, b, c, 1967a, b, 1968) show that stars become brighter and redder as they move away from the zero-age main sequence during core hydrogen burning. Since we are interested in the formation function, $\Psi(M_V)$, the observed luminosity function must be corrected for those evolving stars with spectral types late enough to be assigned the M_V from the next lower bin. The zero-age luminosity function is computed

TABLE 3

FUNDAMENTAL DATA

M_V	$\mathcal{M}/\mathcal{M}_\odot$	ϕ_{MS} ($10^{-4}pc^{-3}$)	$2<\|z\|>$ (pc)	Φ' (pc^{-2})	Φ (pc^{-2})	T (1.5×10^{10} yr.)
-4	26	.0040	100	.000040	.000063	.0006
-3	15	.013	100	.00013	.00017	.0008
-2	9	.063	100	.00063	.00089	.0021
-1	6	.24	100	.0024	.0032	.0043
0	4	.87	120	.010	.014	.011
+1	2.8	2.4	140	.034	.045	.025
+2	2.2	5.8	170	.10	.13	.051
+3	1.6	12	260	.31	.41	.13
+4	1.3	18	360	.65	.58	.27
+5	1.0	36	540	1.9	1.8	.67
+6		46	540	2.5	2.5	

from

$$\Phi(M_V) = \frac{\Phi'(M_V) - c\ \Phi(M_V-1)}{(1 - c)} \qquad (6)$$

where c was determined to be 0.36 for masses down to 1.25 $\mathfrak{M}_\odot$. At that point, the evolutionary tracks tend toward the vertical with negligible color change. For 1.25 $\mathfrak{M}_\odot$, c = 0.13, and for 1 $\mathfrak{M}_\odot$, c = 0. Column 6 shows the corrected luminosity function, and the main sequence lifetimes from Iben (op. cit.) are presented in the last column.

The derived present rate of star formation per square parsec is given in Table 4 and shown graphically in Figure 2. The main sequence lifetimes are sufficiently short for $M_V \leq +2$ that equation (4) was used to compute $\Psi(M_V)$, while the values for fainter magnitudes depend on the choice of models. This combination of data yields a function which, at the bright end, is 3 times larger than that derived by Schmidt (1963). The primary reason is that the factor of 2.5 correction for the contribution of giants to the luminosity function of van Rhijn (1936) is not applicable to that of McCuskey (1966), even though the two functions are nearly identical. Ostriker, Richstone, and Thuan (1974) performed a similar exercise, but obtained an even steeper star formation rate with magnitude, because they claimed that only 12% of the brightest stars are on the main sequence. This value was derived from the luminosity function of Upgren (1963), but his counts were incomplete in that absolute magnitude range, so their value of 12% is probably not correct.

TABLE 4

PRESENT STAR FORMATION RATE

M_V	-4	-3	-2	-1	0	+1	+2	+3	+4	+5	+6	
Ψ ($pc^{-2}/1.5\times10^{10}$ yr.)	.11	.21	.42	.74	1.3	1.8	2.5	3.1	2.1	2.7	2.5	n = 0
								2.8	1.7	1.5	1.0	n = 1
								2.8	1.7	1.2	0.5	n = 2

The white dwarf luminosity function is determined by the rate of star formation on the upper main sequence, and by the white dwarf cooling curve. Recent models have been computed by Lamb and Van Horn (1975) with improved equations of state and explicit treatment of white dwarf crystallization and envelope convection. For $10.0 < M_V < 13.5$, the cooling time from their models may still be adequately approximated by $t_c \propto L/L_\odot^{-5/7}$, or $\log t_c \propto 2/7\ M_{bol}$. (Mestel 1952). Their models for a 1 $\mathfrak{M}_\odot$ pure carbon core were used to set the cooling time scale. New bolometric corrections from Greenstein (1977) allowed conversion to M_V. The relationship is a quadratic, which was approximated by two straight lines

$$\begin{aligned} M_V<11.3 \quad & M_V = 0.34\ M_{bol} + 7.7 \quad \log t_c = .84\ M_V - 11.19 \\ M_V>11.3 \quad & M_V = 0.89\ M_{bol} + 1.9 \quad \log t_c = .32\ M_V - 5.33 \end{aligned} \tag{7}$$

The cooling time expressions scale the result to a mass of 0.7 $\mathfrak{M}_\odot$ and are expressed in units of 1.5×10^{10} years. The modeling process assumes that all stars leaving the main sequence evolve into identical hot white dwarfs that follow this cooling curve. This assumption will be examined further in §V.

Values for the thickness of the white dwarf disk are necessary to convert the predicted surface densities back into volume densities for comparison with the observations. The equivalent width of the disk for a given type of main

sequence star was assumed to be twice the mean z-distance, which increases toward fainter absolute magnitudes, as shown in Table 3. It is further assumed that this increase is correlated with the greater mean age of the fainter stars and reflects a mean z-velocity that grows with time. Stars may add energy to their orbits through several mechanisms, such as binary encounters with massive interstellar clouds as proposed by Spitzer and Schwarzschild (1953), passage through spiral arms, or by experiencing other large-scale fluctuations in the gravitational potential. For purposes of this investigation, the increase in mean z-distance will be described by an empirical relation fit to the data. Using the lifetimes in Table 3, we obtain

$$2\ \langle|z|\rangle = 100 + 700\ t^{.789}\ \text{pc} \qquad (8)$$

which is held at a constant value of 540 pc once that maximum is reached. The form of this relation suggests that the average z-distance for stars of the same age be expressed as a constant plus an exponential growth with time. For a given absolute magnitude, the observed mean z-distance is the average over stars of all ages

$$\langle|z(M_V)|\rangle = \frac{\int_0^{T(M_V)} (z_o + at^p)\,[g(t+1-T(M_V))]^n\ dt}{\int_0^{T(M_V)} [g(t+1-T(M_V))]^n\ dt} \qquad (9)$$

For n = 0 the solution is straightforward

$$\langle|z(M_V)|\rangle = z_o + \frac{a[T(M_V)]^p}{p+1} \qquad (10)$$

which transforms equation (8) to give the growth in mean z-distance with time for any single-age population

$$2\langle|z|\rangle = 100 + 1250\ t^{.789}\ \text{pc} \qquad (11)$$

For the other models, the exact solutions are

$$n = 1 \quad \langle|z|\rangle = z_o + aT^{p+1}\ \frac{\ln 5}{(1-5^{-T})}\ \Gamma(p+1)\gamma^*(p+1, T\ln 5) \qquad (12)$$

where γ^* is the incomplete gamma function, and

$$n = 2 \quad \langle|z|\rangle = z_o + \frac{aT^p}{(p+1)}\ \frac{5}{(5-4T)}\ {}_2F_1\left(2, p+1; p+2; \frac{-4T}{(5-4T)}\right) \qquad (13)$$

where ${}_2F_1$ is the Gaussian confluent hypergeometric function. Happily, power series expansions of equations (12) and (13) produce leading terms identical to that of equation (10) and first order terms that make less than 15% difference for the largest value of T, with higher order terms of alternating sign. Since the analytic g's were approximations in the first place, equation (11) was used to describe the time evolution of mean z-distances for all the models.

For a given white dwarf absolute magnitude, the mean z-distance is the average of the evolved values for all white dwarf progenitors

$$\langle |z| \rangle = \frac{\sum \Psi(M_V) \ [g(1-t(WD))]^n \ [z_o + a(t(WD))^p]}{\sum \Psi(M_V) \ [g(1-t(WD))]^n} \qquad (14)$$

The time spent by the stars in the red giant phase has been neglected, with the age of the white dwarf given by $T(M_V)+t_c(WD)$.

The differential luminosity function itself is calculated by considering the formation of progenitors during the cooling interval defined by the ½-magnitude bins

$$\Phi(M_V(WD)) = \sum \Psi(M_V) \int_{1-T(M_V)-t_c(M_V(WD)-1/4)}^{1-T(M_V)-t_c(M_V(WD)+1/4)} [g(t)]^n \, dt \qquad (15)$$

The sum was truncated above 6 $\mathfrak{M}_\odot$, but the higher masses make a negligible contribution and the results are insensitive to this cutoff.

The models derived are presented in Table 5 and shown in Figure 1 superposed on the data. In regard to Figure 1, it is important to remember that no vertical scaling is possible; the model is a prediction independent of the white dwarf data. The fit is seen to be satisfactory. A formal determination of the "goodness of fit" gives preference to the n = 0 case, although all are acceptable. The absolute level is directly affected by the computed disk thickness, but the limits of the range of mean z-distances allowed by the uncertainties in the data can be no less than a factor of 2. The detailed predictions about the white dwarf disk

TABLE 5

MODEL LUMINOSITY FUNCTIONS

M_V	t_c (1.5×10^{10} yr)	n = 0			n = 1			n = 2		
		$2<\|z\|>$ (pc)	Φ (pc^{-2})	($10^{-3}\phi\ pc^{-3}$)	$2<\|z\|>$ (pc)	Φ (pc^{-2})	($10^{-3}\phi\ pc^{-3}$)	$2<\|z\|>$ (pc)	Φ (pc^{-2})	($10^{-3}\phi\ pc^{-3}$)
9.75	.0010	426			482			517		
			.024	.055		.029	.060		.031	.059
10.25	.0027	432			489			524		
			.057	.13		.069	.14		.074	.14
10.75	.0067	438			496			531		
			.13	.29		.16	.32		.18	.33
11.25	.016	453			510			540		
			.16	.34		.19	.37		.21	.39
11.75	.027	470			526			540		
			.17	.35		.22	.41		.24	.44
12.25	.039	488			540			540		
			.26	.51		.33	.61		.37	.69
12.75	.057	514			540			540		
			.33	.62		.44	.81		.50	.93
13.25	.080	540			540					

therefore have not been strongly tested, although an extremely thin or a halo distribution for the stars in the sample have probably been ruled out. The model is seen to deviate significantly from the data at the bright end. Two factors are contributing. The theoretical cooling curve is very steep for the hottest objects, so that fewer bright white dwarfs may be expected than the $L^{-5/7}$ relation predicts. The absolute magnitude calibration also becomes very insensitive at the hot end, with a 50,000° K temperature range compressed into $0^{m}.04$ in b-y. Small uncertainties in the photometry produce large errors in the absolute magnitude determination, and the probable departure from linearity of the calibration leads to a systematic underestimation of the luminosity when using the linear fit. No correction to the luminosity function has been attempted, but the $M_V = 10.0$ point would be pulled up closer to the model curves.

The model z-distribution can be tested directly by the prediction of counts of hot white dwarfs at fainter apparent magnitudes. With the technique of constructing an m - log π table, the number per square degree of the sky can be computed for any limiting magnitude, given the observed luminosity function and model scale heights. Since the density distributions of main sequence stars can be adequately approximated by $D(z) = e^{-z/z_o}$, this form was assumed to characterize the white dwarf distribution as well, with the

consequence that $z_o = \langle |z(M_V)| \rangle$, as given in Table 5. The difficulty in using this technique of m - log π is that the observed counts must be sufficiently accurate and include a large enough volume to select a meaningfully small range of scale heights from the predictions. The z-distances under consideration must therefore be great enough to indicate densities substantially lower than the local value. The local densities in the luminosity function are not fixed, however, because they were determined for the present sample from volume elements weighted by exponentials with the same scale heights. The net result is a reduction in the sensitivity of the predicted surface densities to changes in z_o, requiring even larger values of z for a significant test.

Sandage and Luyten (1967) give a preliminary list of spectroscopic classifications of a sample chosen for ultraviolet excess. A re-examination of that material produces a sample, with color properties similar to the sample in this investigation, that contains 24 objects, or 0.6 white dwarfs per square degree to a limiting magnitude of 17.75. Because of the similarity in selection by color, the sample was assumed to include all white dwarfs with $M_V < 13.25$; this assumption is not critical since an error in the estimated color limit leading to the exclusion of the last ½-magnitude of the luminosity function would reduce the result by only 10%. The predicted counts are 0.6 per

square degree and are insensitive to the small changes of scale height between the models, with even a factor of 2 decrease in scale height yielding the same result. Although the agreement gives confidence in the present luminosity function, the counts to 18th magnitude do not include sufficient volume to test the model density distribution, and a fainter limit must be sought.

The counts at 20th magnitude can also be predicted, to be compared with work in progress on a plate with that magnitude limit by Schmidt and Ulfbeck (1977). Spectra of 37 ultraviolet excess objects form the basis for a rough preliminary guess of 1 to 2.5 hot white dwarfs per square degree on that plate. To $19^{m}.75$, the model scale heights lead to a prediction of 3.4 per square degree for $M_V <$ 12.75. The as yet uncertain color and magnitude limits make the comparison difficult. The predicted counts go down to 1.6 per square degree if the scale height is made ½ the assumed value. Hence, reliable surface densities of hot white dwarfs at 20th magnitude or fainter will be a powerful test for the density distribution.

A decision about the correct choice of power-law indices, n, in the model may be aided by an estimate of the luminosity function for white dwarfs of fainter absolute magnitudes. Weidemann (1967) noted that the distribution of known white dwarfs was consistent with uniformity out to a distance of approximately 6 pc from the sun. For the

present estimate, we will use 5 white dwarfs with $M_V > 13.25$ known within 6.2 pc: van Maanen's star, G175-34B, L97-12, LP658-2, and G240-72. The resulting space density is 5 per 1000 cubic parsecs for $M_V < 15.7$. The objects were discovered because of their high proper motions; all are greater than $1.5''/a$. The corresponding tangential velocities range from 49 to 68 km/s. On the assumption that the progenitors of these objects were the Population I main sequence stars used in constructing the star formation model, this sample of white dwarfs represents only the high-velocity fraction of the total population in this absolute magnitude range. A rough estimate for a correction may be obtained by considering the fraction of stars with speeds above a specified cutoff in a Maxwellian distribution. This approximation neglects the asymmetry from the solar motion, which produces a larger high velocity tail in the real distribution of tangential speeds. The choice of a value of the cutoff in speed lower than that indicated by the data should help compensate for this underestimate. The computed fraction depends only on the ratio of the cutoff speed to the rms single component of velocity, with the range of this parameter chosen around 1.5. The result suggests that as few as 50% of the total number of white dwarfs within 6.2 pc of the sun with $13.25 < M_V < 15.7$ have been discovered to date. The corrected space density for these objects becomes 10 ± 5 per 1000 cubic parsecs. The star

formation model predicts 11, 18, and 30 per 1000 cubic parsecs for n = 0, 1, and 2 respectively. Although preference is given to the n = 0 model, the difficulties in estimating the large correction preclude the selection of a single value for n. For that value to be determined by white dwarfs alone, an accurate density of the cool degenerates will be required.

As an aside, it is interesting to note that 3 of the 10 nearest white dwarfs of all absolute magnitudes are faint members of multiple systems and would not be detectable in an ultraviolet excess survey, especially at 10 times the distance. This multiplicity factor might explain why the model predictions for the total density in hot white dwarfs exceed the observed value by 30 to 40%.

The model can be used to derive the total local density in white dwarfs. To do that, the total number of upper main sequence stars formed between times 0 and $1-T(M_V)-t_c(13.25)$ is computed. The predicted total densities are given in Table 6, assuming a mean z-distance for cool degenerates of 270 pc and that all white dwarfs may be characterized by a mean mass of 0.7 $\mathfrak{M}_\odot$. From the minimum value of n = 0, degenerate stars account for at least 10% of the mass density in the solar neighborhood (Oort 1965) and represent at least 22% of the number of stars presently on the main sequence (McCuskey 1966). The available data leave open the possibility that the entire unknown mass component of the

TABLE 6

PREDICTED TOTAL DENSITY IN WHITE DWARFS

MODEL n	NUMBER DENSITY ($10^{-3}pc^{-3}$)	VOLUME DENSITY ($\mathfrak{M}_\odot 10^{-3}pc^{-3}$)	SURFACE DENSITY ($\mathfrak{M}_\odot pc^{-2}$)
0	21	15	8
1	50	35	19
2	104	73	39

total local density may be accounted for by degenerate stars.

V. THE WHITE DWARF COLOR-COLOR DIAGRAM

Further direct information about the physical properties of white dwarfs may be obtained from the color-color diagram. Figure 3 plots the Strömgren indices u-b vs. b-y for all stars measured accurately in the course of the observational program, including those fainter objects later dropped from the complete sample. The two indices measure the Balmer jump and Paschen continuum, respectively, for DA stars. A sample of hydrogen white dwarfs of identical composition and surface gravity would therefore define a cooling locus in this plane.

Synthesized colors from model atmospheres by Wickramasighe and Strittmatter (1972) and by Wehrse (1975) have been superimposed on the data. The accuracy of the fit to any given curve can be estimated from the cross, representing the mean measuring uncertainties of $0^{m}.015$ in b-y and $0^{m}.035$ in u-b. The cooler stars seem to be well fit by the log g = 8 models, as found by Weidemann (1975) and Wehrse (1975), but the hot stars show considerable scatter. For the stars between 15,000 and 25,000° K, most of the scatter can probably be explained if the objects near the black body line and the helium model loci are in fact spectral type DB. The classification spectra were often not of

sufficiently high quality to identify weak He absorption features, which would be nearly absent near the black body line. A determination of the distribution of white dwarf spectral types can therefore not be made from this sample, and must be obtained from the work of Sion and Liebert (1977) or Greenstein (1977).

More puzzling is the large scatter of the hottest white dwarfs. Some fraction of the objects are undoubtedly composite, with a redder b-y than the Balmer jump would indicate, but that fraction would be unexpectedly large to account for the number involved. The formal dispersion for the objects hotter than 25,000° K around even the best fit line is twice the measuring uncertainty. Within that uncertainty, they span all the loci between the upper main sequence and the blackbody line. One explanation could be a larger dispersion in log g than previously determined, but Graham's (1972) sample should then have shown more scatter for the cool degenerates. When H^- becomes the dominant source of opacity, the magnitude of the Balmer jump becomes very sensitive to the value of log g, and the tightness of Graham's data suggests a small dispersion in the surface gravity.

Another more cogent explanation involves compositional variations in the cores and remnant atmospheres of the white dwarf progenitors after the red giant phase. If the premise of Van Horn (1968) and Lamb and Van Horn (1975) is correct,

then the phase transition to the solid state adds the latent heat of crystallization to the internal energy and slows the cooling rate. Depending on the internal compositions of the white dwarfs, several crystallization sequences could be formed. Tapia's (1977) observations seem to support this hypothesis, in that they show two distinct sequences of luminosity versus effective temperature, based on models fit to the color indices devised by Wickramasinghe and Strittmatter (1972). The broad band measurements of Eggen and Greenstein (1965), the Strömgren values of Graham (1972), and the monochromatic magnitudes of Greenstein (1977), when plotted as a Balmer jump index versus absolute magnitude, show evidence for more than one cooling sequence. It must be remembered at the same time that the absolute magnitude forms a single sequence with b-y, a measure of temperature for DA stars from the Paschen continuum alone. With the Balmer jump temperature index finding more than one sequence, the possibility must be considered of a range of compositions in DA atmospheres. A variation in the hydrogen to helium ratio from pure hydrogen to that of the extreme DB's might not be unexpected if the evolutionary histories of the progenitors include varying degrees of convective mixing or gravitational diffusion.

The observational evidence makes clear that hot white dwarfs do not fall along a single theoretical cooling sequence. Unfortunately, the spectra of these weak and broad

lined objects do not contain much information about their composition. Perhaps a future look at some of the ultraviolet resonance lines from space will help us begin to unfold this enigma.

VI. SUMMARY

The major results of this investigation may be summarized as follows:

The local luminosity function of hot white dwarfs is presented in Figure 1 and Table 2. The total local density of white dwarfs is 1.43 ± .28 per 1000 cubic parsecs for $M_V < 12.75$.

A model of the local rate of star formation and of disk layer expansion, when combined with white dwarf cooling theory, adequately reproduces the observed luminosity function, as shown in Figure 1. The extension to fainter absolute magnitudes also agrees with observations, although the uncertainties in the data preclude a determination of the change in star formation rate. The model predicts a range of scale heights for hot white dwarfs of 220 to 270 pc, which will be tested by the observed surface density at 20th magnitude. The total local density in degenerate stars expected from the models is at least 20 per 1000 cubic parsecs.

The assumption of a single population of hydrogen white dwarfs with identical composition is not adequate to explain the scatter in the Strömgren u-b, b-y diagram.

The most important conclusion, however, is that the theoretical understanding of main sequence lifetimes and the hot end of the white dwarf cooling curve gives satisfactory agreement with the observational data.

REFERENCES

Arp, H. C. 1965, in Stars and Stellar Systems, Vol. 5, University of Chicago Press, Chicago, p. 455.

Blaauw, A. 1965, in Stars and Stellar Systems, Vol. 5, University of Chicago Press, Chicago, p. 435.

Crawford, D. L., and Barnes, J. V. 1970, A. J., 75, 978.

Eggen, O. J. 1968, Ap. J. Suppl., 16, 97.

Eggen. O. J., and Greenstein, J. L. 1965, Ap. J., 141, 83.

Giclas, H. L., Burnham, R., Jr., and Thomas, N. G. 1971. Lowell Proper Motion Survey, Lowell Observatory, Flagstaff, Arizona.

Graham, J. A. 1970, P.A.S.P., 82, 1305.

———. 1972, A. J., 77, 144.

Green, R. 1976, P.A.S.P., 88, 665.

———. 1977, Ph.D. Thesis, California Institute of Technology.

Green, R., Greenstein, J. L., and Boksenberg, A. 1976, P.A.S.P., 88, 598.

Greenstein, J. L. 1966, Ap. J., 144, 496.

———. 1977, A. J., 81, 323.

Huchra, J. P. 1976, Ph.D. Thesis, California Institute of Technology.

Iben, I., Jr. 1965, Ap. J., 142, 1447.

———. 1966a, Ap. J., 143, 483.

———. 1966b, Ap. J., 143, 505.

Iben, I., Jr. 1966c, Ap. J., 143, 516.

———. 1967a, Ap. J., 147, 624.

———. 1967b, Ap. J., 147, 650.

———. 1968, Ap. J., 154, 581.

Lamb, D. Q., and Van Horn, H. M. 1975, Ap. J., 200, 306.

Luyten, W. J. 1958, On the Frequency of White Dwarfs in Space, Observatory, University of Minnesota, Minneapolis.

Luyten, W. J. 1963-66, Publ. Astron. Obs. Univ. Minnesota, Vol. III, Nr. 13-18.

Luyten, W. J. 1965, First Conference on Faint Blue Stars, University of Minnesota Observatory.

Matsushima, S. 1969, Ap. J., 158, 1137.

McCuskey, S. W. 1966, Vistas in Astronomy, 7, 141.

Mestel, L. 1952, M.N.R.A.S., 112, 583.

Mestel, L., and Ruderman, M. A. 1967, M.N.R.A.S., 136, 27.

Oort, J. H. 1958, Ric. Astr. Specola Vaticana, 5, 415, ("Stellar Populations").

Oort, J. H. 1965, in Stars and Stellar Systems, Vol. 5, University of Chicago Press, Chicago, p. 455.

Ostriker, J. P., Richstone, D. O., and Thuan, T. X. 1974, Ap. J. (Letters), 188, L87.

Rhijn, P. J. van 1929, Publ. Kapteyn Astr. Lab., Groningen No. 43.

Rhijn, P. J. van 1936, Publ. Kapteyn Astr. Lab., Groningen No. 47.

Sandage, A., and Luyten, W. J. 1967, Ap. J., 148, 767.

———. 1969, Ap. J., 155, 913.

Schmidt, M. 1959, Ap. J., 129, 243.

———. 1963, Ap. J., 137, 758.

———. 1968, Ap. J., 151, 393.

———. 1975, Ap. J., 202, 22.

Schmidt, M., and Ulfbeck, O. 1977, private communication.

Sion, E. M., and Liebert, J. 1977, Ap. J., 213, 468.

Slettebak, A., Wright, R. R., and Graham, J. A. 1968, A. J., 73, 152.

Spitzer, L., and Schwarzschild, M. 1953, Ap. J., 118, 106.

Tapia, S. 1977, preprint.

Upgren, A. R. 1963, A. J., 68, 475.

Van Horn, H. M. 1968, Ap. J., 151, 227.

Wehrse, R. 1975, Ay. and Ap., 39, 174.

Weidemann, V. 1967, Zs. f. Ap., 67, 286.

———. 1975, in Problems in Stellar Atmospheres and Envelopes, Springer-Verlag, Berlin, p. 173.

Wickramasinghe, D. T., and Strittmatter, P. A. 1972, M.N.R.A.S., 160, 421.

FIGURE CAPTIONS

Figure 1. White Dwarf Luminosity Function.

For presentation purposes, the data have been grouped into ½-magnitude bins. The error bars represent statistical uncertainties only. The smooth curves are model predictions, labeled by the value of the power-law index, n.

Figure 2. The Present Rate of Star Formation.

Figure 3. White Dwarf Strömgren Color-Color Diagram.

Superposed on the data are model loci, with temperatures given in units of 1000° K. The observational main sequence is from Slettebak, Wright and Graham (1968) and the black body line is from Matsushima (1969). The solid lines connect DA models with log g = 8 and 9 from Wickramasinghe and Strittmatter (1972) while the dashed lines mark hydrogen-deficient models from the same paper. The coolest three points on the log g = 8 curve are due to Wehrse (1975). The cross represents the uncertainty in measurement; note the large scatter in the hottest objects.

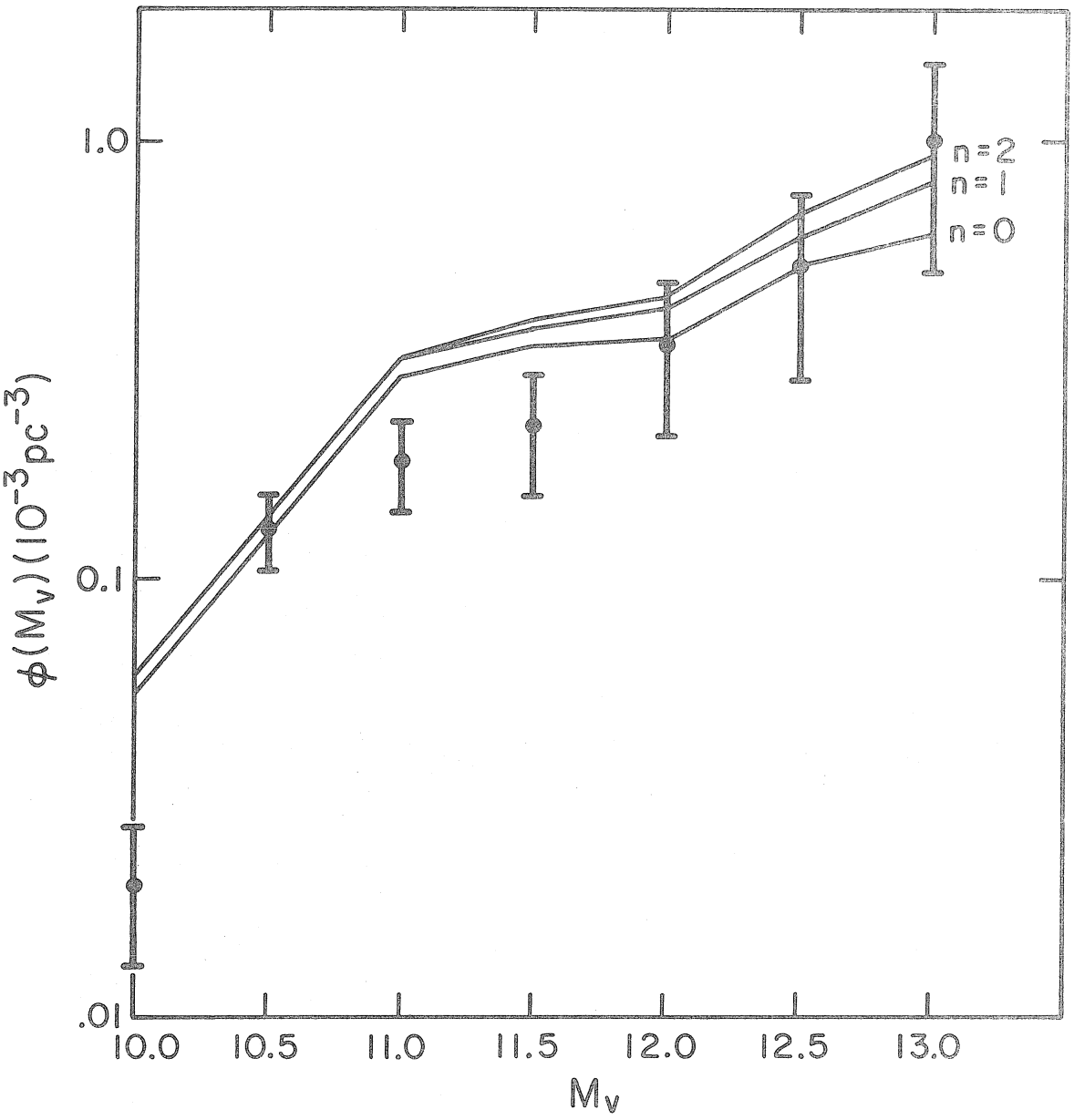

Figure 1

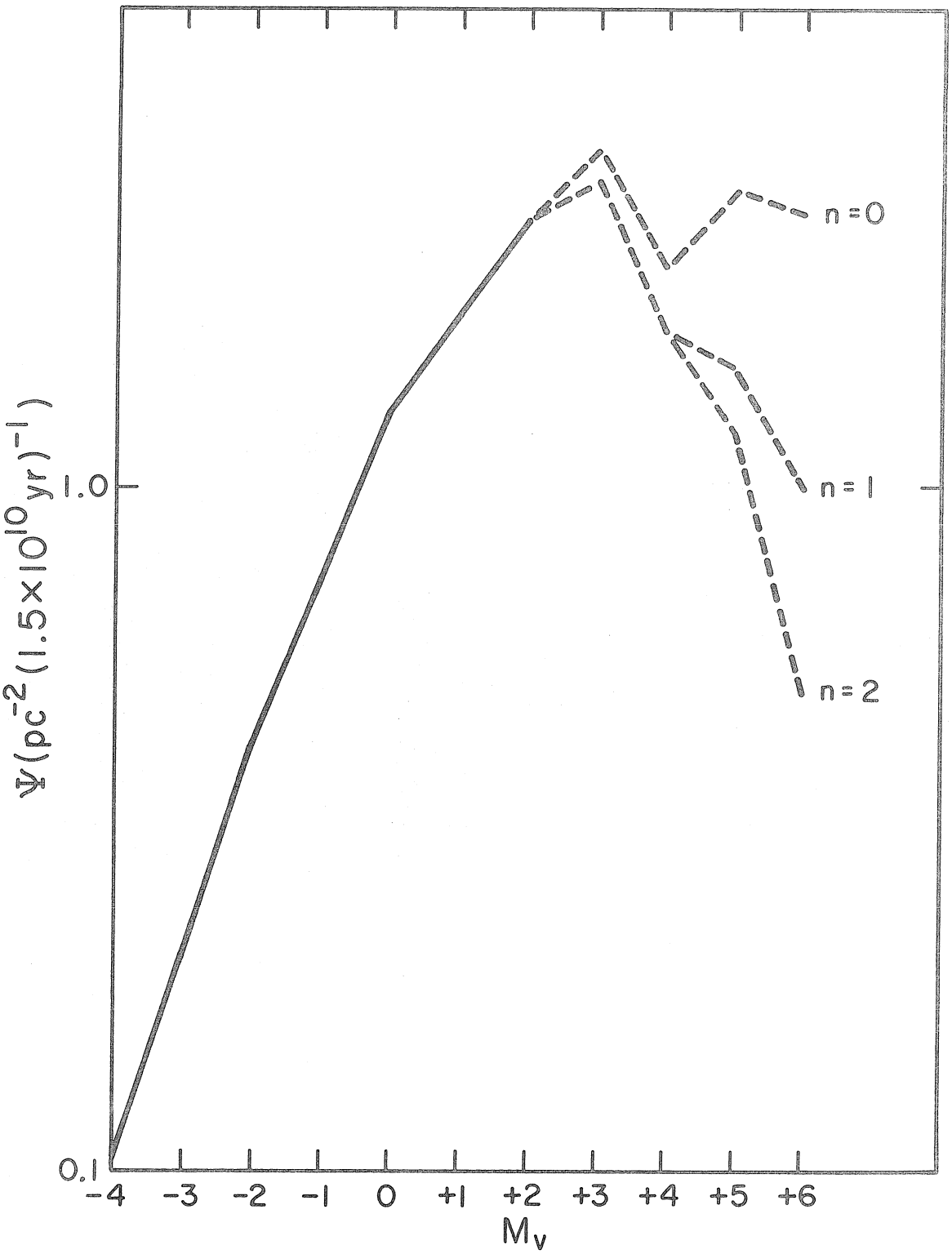

Figure 2

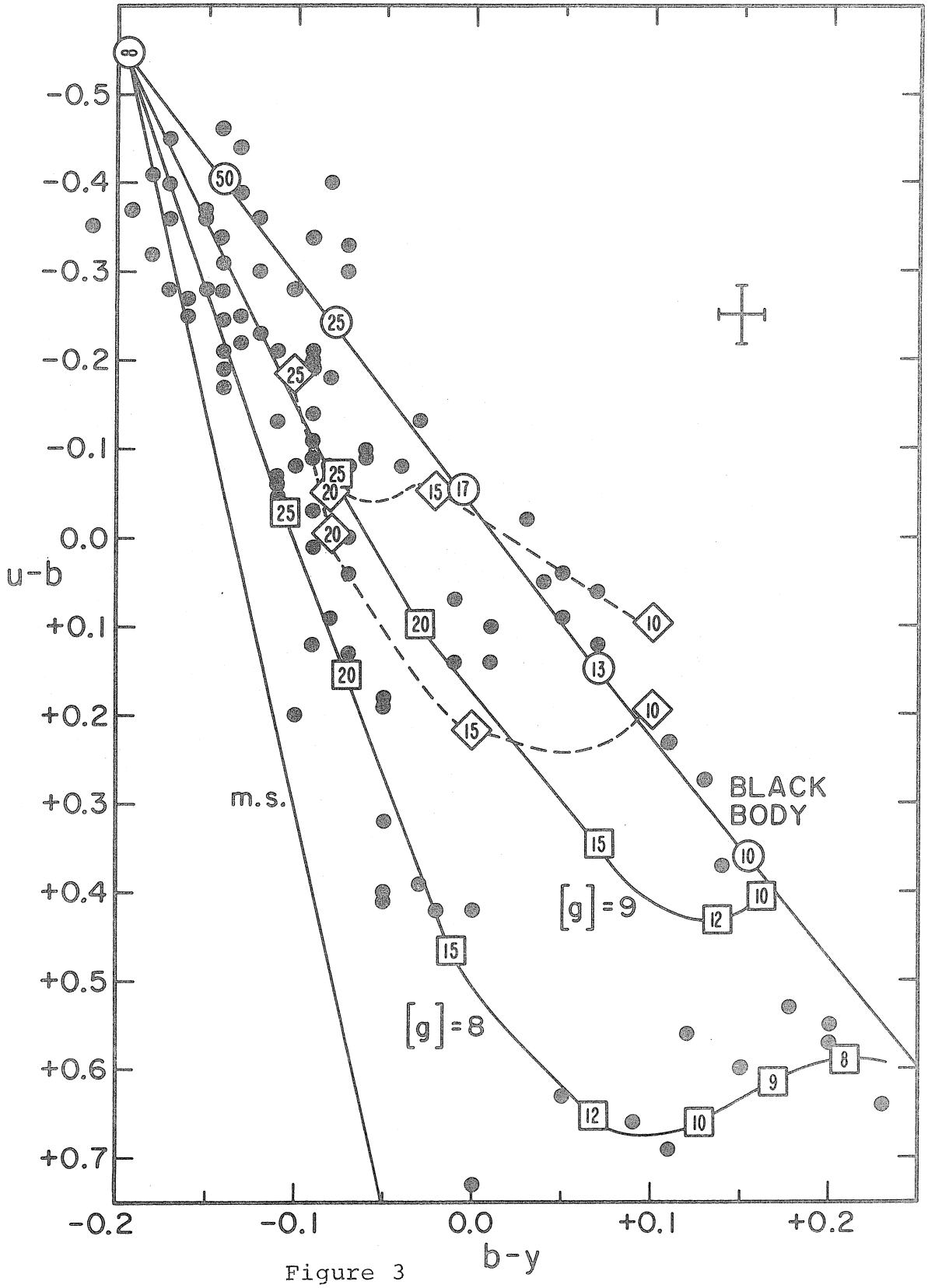
u-b
b-y
-0.5
-0.4
-0.3
-0.2
-0.1
0.0
+0.1
+0.2
+0.3
+0.4
+0.5
+0.6
+0.7
-0.2
-0.1
0.0
+0.1
+0.2
m.s.
BLACK BODY
[g] = 9
[g] = 8

Figure 3

CHAPTER 2

SPECTRAL CENSUS OF A COMPLETE SAMPLE OF FAINT BLUE STARS; LOCAL SPACE DENSITIES OF HOT SUBDWARFS AND QUASARS

I. INTRODUCTION

A photographic two-color survey has been undertaken to isolate a complete sample of objects selected for ultraviolet excess (Green 1976). Spectroscopic classification of candidates is now essentially complete over a limited area of the survey, and a preliminary determination may be made of the space densities of hot subdwarfs and quasars. The evolutionary status of the hot subdwarfs is highly uncertain (see, for example, Newell 1973, Greenstein and A. Sargent 1974, Iben 1974), so it is hoped that this information will be of some aid in evaluating theoretical predictions. The local space density of quasars is derived on the assumption of a cosmological origin for their redshifts. This density is useful for comparison with the luminosity function of Seyfert galaxies and with models for the density evolution of quasars (Schmidt 1970).

The ultraviolet excess objects were chosen to have $U-B < -0.5$ and were selected from 26 films taken on the Palomar 18-inch Schmidt telescope, covering an area of 1434 square degrees above $|b| = 37°$. All were then observed spectroscopically, either on the Palomar 1.5-meter telescope at an inverse dispersion of 280 Å mm^{-1}, or by Dr. Maarten Schmidt on the 5-meter telescope at 190 Å mm^{-1}. The crucial quantity in the definition of a complete sample for statistical study is the limiting magnitude. The completeness limits

for these films were determined by a careful application of the V/V_m test (Schmidt 1968) to the large sample of hot white dwarfs identified in the same fields (Green 1977). The resulting magnitude limits are expected to be accurate to within $0^m.1$.

A breakdown by spectral type is presented in Table 1. The strongly predominant constituent of the faint blue stars down to the mean limiting magnitude of B = 15.7 is seen to be the hot white dwarfs. The table includes the previously known white dwarfs, subdwarfs, quasars, and compact galaxies; the sample was limited to star-like objects, however, and does not include objects obviously extended at the scale of the discovery films, such as blue galaxies or planetary nebulae. The cataclysmic variable is PG 2337+12, as discussed by Green, Greenstein, and Boksenberg (1976). The helium and peculiar stars will be the subject of a future investigation.

The local space densities were derived using a method discussed by Schmidt (1975). The contribution of each object to the total density is $1/V_m$, where V_m is the volume of space available to the object within which it would still appear in the magnitude-limited sample. The total maximum volume is the union of the maximum volumes found for each field individually. The total local density for a given spectral type is then the sum of the contributions of all objects in the sample of that type.

TABLE 1

BREAKDOWN BY SPECTRAL TYPE

Number	Type
81	White dwarfs
9	Subdwarf B
8	Subdwarf O
4	Quasars
4	Compact or Seyfert galaxies
2	Helium Stars
1	Cataclysmic Variable
6	Peculiar

The result thus obtained is the mean density over the sampled volume. The local density will be different from this value in the presence of a non-uniform space distribution. For the hot subdwarfs, only mean densities were computed, since their density distribution as a function of distance from the galactic plane is not known. The discussion of these objects will be found in §II. The quasar space density distribution has been found to be strongly non-uniform (Schmidt 1968). The consequent modification of the $1/V_m$ method and the results will be presented in §III.

II. HOT SUBDWARFS

Precise classification of low-dispersion image tube spectra is difficult. Working definitions for spectral types of faint blue stars have been given by Sargent and Searle (1968) and Greenstein and A. Sargent (1974). These classifications depend on an accurate impression of line widths and of intensities for some weaker lines, about which a judgment is difficult to make from lower quality spectra. In particular, a substantial group of the spectra under consideration show only relatively sharp hydrogen Balmer absorption, with lines beyond the confluence of the series for white dwarfs on spectra of the same dispersion.

Some a priori knowledge of the temperature range is helpful in deciding what these objects are. The selection cutoff in U-B is known; the broad-band photometry of faint

blue stars by Eggen and Sandage (1965) suggests that this limit corresponds to a limit in the reddening-free parameter Q (Johnson and Morgan 1953) of ~ -0.6. Hyland's calibration of Q, as quoted by Greenstein and A. Sargent (1974), leads to a lower limit in effective temperature of 18,000° K. Stars hotter than this temperature with broadened hydrogen lines fall into Newell's (1973) class Horizontal Branch "D" or Greenstein and A. Sargent's (1974) region of subdwarf B. The line profiles and low visibility of the helium lines on the image tube spectra cannot rule out the possibility that these are main sequence B stars; the sample, however, has a mean limiting magnitude of B = 15.7, and the density of run-away B stars at distances greater than 10 kpc above the plane is probably very low.

To find the maximum distance at which a given subdwarf B star could still be contained in this magnitude-limited sample, its absolute magnitude must be known. Greenstein and A. Sargent used observed line strengths and photoelectric colors in combination with model atmospheres to derive surface gravities and effective temperatures for the stars in their lists. The light to mass ratio is then proportional to T_{eff}^4/g. By assuming a mass for Population II horizontal branch stars and bolometric corrections from the model atmospheres, they arrived at a mean $M_V = +3.1$ for the subdwarf B stars, with a dispersion of less than a magnitude. This absolute magnitude was assigned to all the

subdwarf B stars, along with a mean B-V to compute maximum volumes based on the B magnitude limits of the films. The method described in §I yields a local mean density of subdwarf B stars of $(1.4 \pm .5) \times 10^{-9}$ pc^{-3}. The quoted error is the statistical uncertainty from the number of objects in the sample.

This is the first estimate of the mean space density of subdwarf B stars based on a complete spectroscopic sample. A preliminary answer may now be offered to the question of why a number of these stars have been discovered in the field halo population, yet only one has ever been found in a globular cluster. An estimate may be made of the fractional contribution of the horizontal branch to the total number of halo stars from the luminosity function of the globular cluster M3 by Sandage (1953). His data show a clearly delineated hump in the luminosity function caused by blue horizontal branch stars, that includes approximately 1% of the total number of stars for $M_{pg} < 7.5$. The mean local density of all extreme halo stars was determined by Schmidt (1975) from a sample of objects with high tangential velocities. That sample contains 3 stars with $M_{pg} < 7.5$, corresponding to a mean local density of such halo stars of $\sim 3 \times 10^{-4}$ pc^{-3}, after correction for multiplicity. The resulting mean density in horizontal branch stars is $\sim 3 \times 10^{-6}$ pc^{-3}. The consequence is that subdwarf B stars comprise only .0005 of the number of stars on the blue

horizontal branch of the extreme halo; this value would be an upper limit for all field Population II stars. The fact that only one has been observed in globular clusters is therefore not surprising, and cannot be considered as evidence for a basic difference between halo field and globular cluster populations. The observed density of subdwarf B stars must represent a combination of progenitor density and evolutionary lifetime that makes these objects rare in comparison with the blue horizontal branch.

The spectroscopic classification of the hotter subdwarf O stars is more reliable than for the subdwarf B's. These objects show absorption from He II λ4686 and several neutral helium lines, with the newly discovered members of this sample showing no evidence for hydrogen absorption at low dispersion. The absolute magnitude calibration for these objects is much more difficult, however, because of the strong helium lines, the near absence of hydrogen lines, and the paucity of accurate models at very high effective temperatures and subdwarf surface gravities. Greenstein and A. Sargent (1974) discuss these problems in detail; $\langle M_V \rangle = +4.0$ has been adopted for the subdwarf O stars as an average of their value and that obtained by Luyten (1976) from kinematic arguments, with the understanding that the cosmic dispersion is more than 2 magnitudes. The resulting space density is $(3.4 \pm 1.2) \times 10^{-9}$ pc^{-3}; the value scales as $10^{0.6\ M_V}$.

This density makes unlikely the possibility that these stars have a direct evolutionary connection with the observed hot white dwarfs or planetary nebulae, even though they populate a pivotal region of the H-R diagram. The density of the hot white dwarfs is $\sim 1 \times 10^{-4}$ pc^{-3} (Green 1977), which represents $\sim .001$ of the total local star density (McCuskey 1966). The total local density of the extreme halo is $\sim 1 \times 10^{-3}$ pc^{-3} (Schmidt 1975), so the observed hot white dwarfs are nearly pure disk population. If subdwarf O stars were the immediate progenitors of these hot white dwarfs, then the ratio of their densities would give the ratio of the evolutionary time-scales. The white dwarf cooling times from models of Lamb and Van Horn (1975) force a solution for the lifetime of the subdwarf O's of $\sim 10^3$ years. This result is in contradiction with their value of $\sim 10^6$ years for the time required for the stars to cool from their mean absolute magnitude to the one at which they would begin to be classified spectroscopically as white dwarfs. One solution is that the mean absolute magnitude adopted for the sdO's is too bright, leading to a derived space density that is too low. To approximate the model cooling time from the ratio by a sufficient increase in space density, the adopted mean absolute magnitude of the subdwarf O's would have to be made fainter by about 5 magnitudes to $\langle M_V \rangle \geq +9$, close to that of the hot white dwarfs themselves. The line profiles of the subdwarf O stars are not compatible with

the surface gravities expected for stars of this brightness on the cooling sequence. This chain of reasoning leads to the conclusion that the observed subdwarf O stars are not representative of the progenitors of the observed hot white dwarfs.

A similar argument may be applied to the planetary nebulae. Their observed density is $\sim 5 \times 10^{-8}$ pc^{-3} (Cahn and Kaler 1971). If the nuclei are the direct progenitors of the sdO stars, then the planetary nebular lifetime of $\sim 2 \times 10^{4}$ years (Salpeter 1976) forces the subdwarf O lifetime to be $\sim 10^{3}$ years, again in disagreement with model cooling times. Both planetary nebulae, because of their concentration to the galactic plane, and hot white dwarfs are members of the disk population. One possibility for the subdwarf O stars is that they have no evolutionary connection to the former two types of extreme temperature objects, but rather belong to the halo and are in a well-defined but unknown evolutionary state, similar to the subdwarf B stars. Another less tractable alternative is that the designation subdwarf O encompasses a more diverse group of high temperature stars, possibly of mixed population, that represent only a small fraction of "normally" evolving objects.

The general conclusion to be drawn from the derived space densities is that the hot subdwarfs comprise less than .001 of the halo horizontal branch, and must reflect some combination of a limited population of progenitors and a

brief evolutionary lifetime.

III. QUASARS

The spectroscopic observations have produced a very small but statistically complete sample of 4 quasars, from which the local space density may be estimated. The assumption is made that the redshifts of these quasars are of cosmological origin, and may be used as an indicator of distance. For comparison with earlier work by Schmidt (1968 1970, 1972), the densities are computed per unit co-moving volume using a deceleration parameter $q_o = 1$, to make the luminosity distance scale as z. The results are insensitive to this choice of q_o, especially since the maximum z of the sample is less than 0.5.

Three density distributions are considered. The first is a uniform distribution for reference, for which the computational procedure is identical to that described in §I. Schmidt (1968) found, however, that the space density of quasars is a steeply increasing function of redshift. To derive the local density in the presence of a non-uniform distribution, it is necessary to weight each differential volume element by the normalized distribution function, so that $dV' = dV\ D(z)$. Schmidt (1970) used two forms of the increase in density that fit the change in counts between 17th and 18th magnitudes: $D(z) = (1+z)^6$ and $D(z) = 10^{5\tau}$ where τ is the fractional cosmic look-back time. The local

densities of quasars derived under the three assumptions are presented in Table 2; a value of 50 km s^{-1} Mpc^{-1} was used for the Hubble constant.

These results are in reasonable agreement with those of Schmidt (1972), who determined the local density of quasars from a much larger sample of optically selected quasars at 18th magnitude. For a Hubble constant of 50, his luminosity functions give the predicted values in Table 2. The trend of the numbers reflects the steepness of the weighting functions. It is of interest to compare the local density of quasars with the luminosity function of Markarian Seyfert galaxies, as determined for a uniform space distribution by Huchra and Sargent (1973). The least luminous quasar in the present sample would fall in their brightest absolute magnitude interval; the contribution to the space density of the two objects in that one-magnitude bin is 36 Gpc^{-3}. The low luminosity quasar represents $\sim$ 80% of the observed density in Table 2. The conclusion to be drawn is that, on the assumption of cosmological redshifts and considering the very large uncertainties, the luminosity function of quasars joins smoothly, albeit steeply, with the luminosity function of Markarian Seyfert galaxies. In other words, the space densities provide no contradiction to the hypothesis of a smooth transition between the phenomena of Seyfert galaxy nuclei and quasars.

TABLE 2

LOCAL SPACE DENSITY OF QUASARS
(GPC^{-3})

Density Law	$D = 1$	$D = (1+z)^6$	$D = 10^{5\tau}$
Observed	34 ± 24	17 ± 13	4.5 ± 3.9
Predicted		13	1.1

The surface density at bright apparent magnitudes is a powerful determinant of the choice of density laws (Green 1976). Schmidt's (1972) luminosity function for quasars was used with the m - log z technique to predict the expected number of objects in the present sample. The two density laws give 4.8 for $D = (1+z)^6$ and 2.0 for $10^{5\tau}$. The observed result of 4 ± 2 is consistent with either distribution, and the uncertainties are as yet too great to make a definite choice. It is hoped that further discovery work now under way will resolve this question.

REFERENCES

Cahn, J. H., and Kaler, J. B. 1971, Ap. J. Suppl., 22, 319.

Eggen, O. J., and Sandage, A. 1965, Ap. J., 141, 821.

Green, R. F. 1976, P.A.S.P., 88, 665.

———. 1977, Ph.D. Thesis, California Institute of Technology.

Green, R. F., Greenstein, J. L., and Boksenberg, A. 1976, P.A.S.P., 88, 598.

Greenstein, J. L., and Sargent, A. I. 1974, Ap. J. Suppl., 28, 157.

Huchra, J., and Sargent, W. L. W. 1973, Ap. J., 186, 433.

Iben, I., Jr. 1974, Ann. Rev. of Astron. and Ap., 12, 215.

Johnson, H. L., and Morgan, W. W. 1953, Ap. J., 117, 313.

Lamb, D. Q., and Van Horn, H. M. 1975, Ap. J., 200, 306.

Luyten, W. J. 1976, Proper Motion Survey, 45, University of Minnesota.

McCuskey, S. W. 1966, Vistas in Astronomy, 7, 141.

Newell, E. B. 1973, Ap. J. Suppl., 26, 37.

Salpeter, E. E. 1976, Ap. J., 206, 673.

Sandage, A. 1953, Ph.D. Thesis, California Institute of Technology.

Sargent, W. L. W., and Searle, L. 1968, Ap. J., 152, 443.

Schmidt, M. 1968, Ap. J., 151, 393.

———. 1970, Ap. J., 162, 371.

———. 1972, Ap. J., 176, 273.

———. 1975, Ap. J., 202, 22.

CHAPTER 3

AN AUTOMATED TECHNIQUE FOR STELLAR MAGNITUDE, COLOR, AND POSITION MEASUREMENTS OF ASTRONOMICAL PHOTOGRAPHS

I. INTRODUCTION

The observational material has been obtained for a photographic two-color survey of 10,000 square degrees of the sky at high galactic latitude (Green 1976). The purpose of the survey is to isolate a complete sample of stellar objects showing an ultraviolet excess in U-B, which provides a list of candidates for spectroscopic classification into quasars, white dwarfs, and halo stars for statistical study. The completeness limit of the sample is expected to be around 16th magnitude in the blue. Finishing the project would therefore require the examination of some 5 million image pairs and the measurement of 3000 to 5000 candidates for position, magnitude, and color. Performance of this task by traditional methods would be both tedious and prone to significant subjective error in selection of objects.

Computer-assisted inspection and measurement of the films are the means to an objective and consistent treatment of the data. The Image Processing Laboratory of the Jet Propulsion Laboratory has provided the facilities for the project, both for digitization of the films on their PDS scanning microdensitometer and for reduction of the digital images by batch programs compatible with VICAR, the executive-level language designed for convenient manipulation of large disk data sets. Significant success has already been reported in using the PDS microdensitometer for measuring stellar positions (Chiu 1976) and magnitudes (Herzog and

Illingworth 1977). The programs described here were written to make the most effective compromise among speed, accuracy and data handling efficiency. Film measurement and a real-time image detection technique will be discussed in §II, the program for image consolidation and pairing in §III, photometry and position measurement in §IV, further modifications and applications in §V, and the results will be summarized in §VI.

II. FILM MEASUREMENT AND REAL-TIME IMAGE DETECTION

The data base of the two-color survey consists of 280 films taken on the Palomar 18-inch Schmidt telescope. The primary goal of the project is to develop the capability of processing this number of films with one-pass digitization and reduction. The emulsion type chosen was IIa-O, both for its spectral response, and as a compromise between speed and resolution (Kodak 1973); the usable field is a circular area 14.2 cm. in diameter. The angular scale of 220 arc-seconds per millimeter places a severe constraint on the scanning aperture and therefore on the total scanning time. The parameters chosen were a 20μ round scanning aperture and a 10μ step. The use of this relatively large aperture is equivalent to the application of a low-pass filter that excludes spatial frequencies higher than $1/20\mu^{-1}$. The film grain noise is so substantial at twice that frequency that the star finding algorithms were unable to function on data

scanned with a 10μ aperture. The grain noise averaging also helps reduce the number of single pixel spikes that are detected as spurious images. The corresponding resolution of 4".4 is adequate for two reasons. The 18-inch Schmidt corrector is optimized in the blue, so that even at best focus, the ultraviolet images are "soft". The blue exposures were defocused, both to match the quality of the adjacent ultraviolet exposures and to decrease the steepness of the curve of stellar image growth with magnitude. These films therefore contain little information on scales of less than 4". Likewise, no spatial reconstruction of the image is ever attempted, so that the loss of higher spatial frequencies is not a relevant consideration.

The digitizing system at the Image Processing Laboratory is a PDS 1010G scanning microdensitometer with a dynamic range of 4 density units, controlled by a PDP8 minicomputer with 8 K of core. The extreme stability of the granite stage and lead screw places the scanning speed limit on the electronics, in particular, the log amplifier. Knife-edge scans show that the response time of this amplifier is inadequate even at the slowest carriage speed. The result is that, although the linear optical encoders provide positions accurate to 1μ, the density level is systematically altered by the brightness of the area just scanned. Since the film scans were to be made in raster mode, the single line edge distortion and centroid shift of brighter

(i.e., larger) images average out. The scanning rate and step size were therefore chosen by studying the accuracy of faint stellar magnitude determinations. The average uncertainty in magnitude remains nearly constant up to 6 kHz, so 5.5 kHz was chosen as the data acquisition rate, and oversampling with a 10μ step did reduce the uncertainty.

With this data rate and scanning step, a 14.2 cm. square area can be scanned in raster mode in 11 hours. The storing and manipulation of the 200 million pixels for processing on even a large computer is not practical, however, so a means of data compression was sought. It is certainly true that there is no information outside the inscribed circle, so that 4-π of the pixels can be immediately rejected. The further assumption was made that the sky background is useful only as a reference level, with the consequence that it must be monitored locally, but not stored for later processing. A real-time threshold routine was therefore written for the minicomputer control system, that records on magnetic tape only those pixels within the density enhancements of stellar and other images. Two threshold levels are set for each film: the first is a mean photographic density for sky at the edge of the film. Pixels with densities less than this lower sky threshold are simply rejected. The second threshold is the density level above mean sky at which the enhancement is sufficient to be considered a detection of an object. A box filter is applied

to the sky background by computing a running average of 16 consecutive pixels, and each new pixel is tested against the second threshold. A new sky value with density difference less than the threshold is included in the average after the oldest one is dropped. When a stellar image is encountered, the density of each pixel is recorded on magnetic tape along with the corresponding x-coordinate. When the density difference drops below the threshold, the sky averaging procedure is resumed. A successful compromise between faint limiting magnitude and spurious detection of noise peaks was found at a threshold level of $2\frac{1}{2}\sigma$ above the r.m.s. sky noise, at about 0.3 PDS density units.

There are two major advantages to this real-time threshold routine. The first is that it affords a data compression of over a factor of 100, allowing the data from all 14,200 lines to fit easily on one 2400-foot reel of magnetic tape. A corollary to this saving is that the image detection is essentially free, because it does not involve array manipulation during the batch processing. The other advantage is that it provides a consistent definition of the image boundary with respect to the local sky level, so that magnitudes can be determined in a uniform way. No attempt was made either to convert photographic densities to intensities or to subtract the sky level from the density values of pixels within stellar images. The power in the low frequencies of the background noise is low with this telescope,

filter, and film combination, so that this large-scale uniformity allows an accurate stellar magnitude measurement from photographic density alone.

III. IMAGE CONSOLIDATION AND PAIRING

Two programs have been written for the Image Processing Laboratory's I.B.M. 360/65 computer to reduce the raw data obtained from the PDS scanner. The programs are compatible with VICAR, the job control level image processing language (VICAR 1971). Existing software could therefore be utilized for simplified and efficient binary tape reading and manipulation of large disk data sets.

The specific goal of the data reducion is to obtain accurate magnitudes, colors, and positions for stars in a 4 magnitude range starting at least $0^{m}.2$ brighter than the blue magnitude limit of the film. This goal alleviates three major computational difficulties described by other workers: the program does not attempt to distinguish faint stars from noise at the absolute limits of detection (Sebok 1977); it does not try to deal with saturated images of brighter stars adorned with diffraction spikes and halos (Herzog and Illingworth 1977) (they are assumed to be contained in other catalogues); and the program does not attempt to measure accurate magnitudes and colors for extended objects (Oemler 1974), although they are classified and positions determined.

The computational philosophy of the first program is line-by-line condensation of images into weighted delta functions, line-to-line correlation of slices of the same image, then pairing the completed ultraviolet and blue images of each star. Figure 1 shows a graphical representation of this process. In particular, the entire tape is logged to disk and the PDS line headers are removed after extracting the information about the number of pixels in the line and the y-coordinate, then each line of data is read into core individually to be processed. A stellar image slice is identified as consisting of a string of density values with consecutive x-coordinates. Three quantities are derived for each image slice: the integrated optical density, that is, the sum of the densities for all the pixels in the line image; a density-weighted x-centroid; and a slope parameter, which is the central density divided by the image radius.

In the case of bright stars or close spacing between the ultraviolet and blue images, they will overlap and appear as one long data string. A matched filtering technique has been devised to split data arrays that are at least as long as the x-distance between U and B images. The filter is a pair of broad Gaussians with the correct separation and self-scaled in relative peak value by density samples taken from either end of the data string. This filter is cross-correlated with the image array and the

displacement of the maximum value from the edge fixes the position of the peaks. The absolute minimum between the peaks is located, and defines the boundary between the pair of images in that line.

Occasionally, extremely extended objects are encountered, such as large galaxies, first magnitude stars, or labeling information from the edge of the film. In these cases, when the data string is longer than 1½ arcminutes, the image is not filtered but is consolidated into one image, because the color cannot be measured by this technique.

Each line of scanner data is read in and processed in the same way, then compared to an array of "active" stars under reconstruction. If the x-centroids of a new image slice and an active image agree to within the tolerance imposed by image asymmetry and log amplifier response, they are combined. The total densities are added, and a new density-weighted x-centroid, y-centroid, and slope parameter are computed, after which the star is returned to the active file. If a star image has had no additions for 2 lines, it is considered completed and moved to a final storage array with capacity for 90,000 stars. A careful search is conducted to find the corresponding image of the other color, including tests for overlapped pairs. The final storage array contains five items of information on each star: x and y-coordinates and slope parameter for the blue image,

instrumental B magnitude and U-B color. The entire image consolidation phase, including tape logging, requires only 170 K of core and takes less than 12 minutes of CPU time, so it is felt that the goal of relative efficiency in computation has been achieved.

IV. PHOTOMETRY AND POSITION MEASUREMENT

The second program transforms the instrumental quantities to values on standard systems. The instrumental positions of a grid of stars with accurate equatorial coordinates (Smithsonian 1966) and of several faint stars measured photoelectrically on the UBV system are recorded prior to the scanning of each film, and given to the program as parameters. The program searches the final storage arrays for the photoelectric standards and presents the user with the instrumental values retrieved as well as a set of transformation equations. Because of the limited magnitude range of interest and the limited availability of photoelectrically measured faint stars at high galactic latitude for any given field (a list of sources used for stars fainter than 12th magnitude may be found in the bibliography), a linear transformation is derived for both the B magnitude and the U-B color. A color term is explicitly calculated to take into account the differences in bandpasses between the film and filter combinations (IIa-O + Schott GG 13 and UG 2) and the standard system. This term, when averaged over a number of fields to remove fluctuations in the fit, is small,

amounting to a systematic change of no more than $0^m.15$ in U-B over a 4 magnitude range in B.

The internal accuracy achieved is $0^m.19$ in B and $0^m.09$ in U-B. This result is to be compared to $0^m.05$ in magnitude achieved by Herzog and Illingworth (1977), while considering the difference of a factor of 10 in both plate scale and the number of standards per plate. The higher accuracy in the color fit is a result of the facts that the color is a local differential measurement, so that focus and film sensitivity variations are minimized, and that the magnitude fit as given does not contain a correction for color. Any remaining systematic differences from field to field are removed by using suitably averaged slopes and color terms and adjusting zero points, for magnitude by considering the total number of stars detected per unit area and for color by including extinction corrections and by forcing consistent results for overlapped regions of adjacent fields.

Once the photometric transformations have been derived, the magnitude and color for each star on the film is determined. Stars can be selected for any range of photometric properties; in this case, for U-B<-0.4. The position on the sky for every star selected is then computed using the method of dependence (Comrie 1929). Rather than solving for a global fit for the entire grid of 8 to 10 position standards, the program chooses the three closest to the unknown as the local reference system, a procedure that is

computationally simpler and more accurate in the present case. The instrumental coordinates used for the bright position standards were those found by precise positioning of the stage prior to the scan, because the image condensation program is not accurate in determining the centroids of saturated, overlapped image pairs with diffraction and reflection features. The positional accuracy of the program was determined by comparison of the results for a sample of faint stars to their true positions, known to 1 arcsecond. The total mean error in a single measurement is no more than 4.5 arcseconds, the predicted resolution of the data. These positions are adequate for preparation of observing material and comparison of candidates with lists of known ultraviolet excess objects.

The final phase of the program is output. A catalogue is printed with the celestial coordinates, magnitudes, colors, and 5 instrumental parameters for all stars selected. A digital picture is generated which produces an overlay finding chart to scale for the 18-inch film, allowing the user to examine the objects. An example is presented in Figure 2. As a by-product of the search procedure a histogram is computed of the number of stars per one-tenth magnitude interval in B, along with the total number of objects detected. This latter number is relatively free of confusion from plate defects, because the only objects counted are those with both U and B images. The shape of

the histogram and the total number detected can be used to give an accurate determination of the limiting magnitude of the film. The capability also exists of creating a graphical color-magnitude histogram for use in cluster work.

V. FURTHER MODIFICATIONS AND APPLICATIONS

The program as it stands is a powerful tool for selecting a class of stellar objects based on color and magnitude; out of 20,000 stars in a typical field, it will isolate 200 with ultraviolet excess for visual inspection. The major remaining source of confusion in the identification of objects is blended images. In gaining the great efficiency of line-by-line processing, the ability to utilize the power of two-dimensional gradient techniques as described by Herzog and Illingworth (1977) is lost. At high galactic latitude, the problem is not major, however, and the recognition of irregularity in the double image pattern could be further exploited.

Star-galaxy differentiation has not yet been pursued in detail. It was found in this study, as by Oemler (1974) and Herzog and Illingworth (1977), that for brighter objects the two classes are easily distinguished in a plot of integrated density versus slope parameter. For this data base, the ability to discriminate decreases more rapidly with magnitude because of the smaller plate scale and the fact that the stellar images were defocused. The data may be suitable for statistical studies of galaxy clustering, but

the magnitude of brighter objects cannot be accurately determined without a conversion to intensity, and the uncertainties in identification at the faint end would probably produce a completeness limit comparable to that of the Zwicky sample (Zwicky, et al. 1961-68). Nevertheless, the coverage of 10,000 square degrees of the sky makes this investigation worth considering.

The program itself has general application. It has been used to reduce two-color plates from the 48-inch Schmidt telescope, since questions of scale and dimension are all under parameter control. Other uses include the reduction of multi-color plates with three or more images, and more accurate work on single-image plates of greater angular scale with more sophisticated photometric conversions.

VI. SUMMARY

A series of computer programs have been written for the acquisition and reduction of data from astronomical photographs digitized on a PDS scanning microdensitometer. The techniques of real-time threshold object detection and line-by-line image consolidation for single-pass digitization afford a great saving in computing time. The programs were written to isolate a complete sample of ultraviolet excess objects from a two-color sky survey taken on the Palomar 18-inch Schmidt telescope. The films were scanned at 4".4 resolution; density-weighted centroids yield positions on the

sky accurate to 4".5. Linear fits of the integrated optical density to photoelectric standards give mean accuracies of $0^m.19$ in B and $0^m.09$ in U-B on a single film. These programs will provide an objective means for examining five million image pairs over 10,000 square degrees of the sky and isolating three to five thousand ultraviolet excess objects for spectroscopic identifications of a complete sample of bright quasars, white dwarfs, and halo stars.

REFERENCES

Chiu, L.-T. G. 1976, P.A.S.P., 88, 803.

Comrie, L. J. 1929, J.B.A.A., 39, 203.

Green, R. F. 1976, P.A.S.P., 88, 665.

Herzog, A. D., and Illingworth, G. 1977, Ap. J. Suppl., 33, 55.

Kodak Plates and Films for Scientific Photography, 1973, Eastman Kodak Company, Rochester, New York.

Oemler, A. Jr. 1974, Ap. J., 194, 1.

Sebok, W. 1977, private communication.

Smithsonian Astrophysical Observatory, 1966, Star Catalog, Smithsonian Institution, Washington, D. C.

VICAR, Guide to System Use, 1971, Jet Propulsion Laboratory, Pasadena, California.

Zwicky, F., Herzog, E., Wild, P., Karpowicz, M., and Kowal, C. T. (1961-1968) Catalogue of Galaxies and Clusters of Galaxies, California Institute of Technology, Pasadena, California.

REFERENCES FOR PHOTOMETRY OF FAINT STARS

Angione, R. J. 1971, A. J., 76, 413.

Bern, K., and Wramdemark, S. 1973, Lowell Obs. Bull., 8, 1.

Eggen, O. J. 1968, Ap. J. Suppl., 16, 97.

Eggen, O. J., and Greenstein, J. L. 1965, Ap. J., 141, 83.

———. 1967, Ap. J., 150, 927.

Eggen, O. J., and Sandage, A. 1965, Ap. J., 141, 821.

Giclas, H. L., Burnham, R., and Thomas, N. G. 1971, Lowell Proper Motion Survey, Lowell Observatory, Flagstaff, Arizona.

Green, R. F. 1977, unpublished.

Greenstein, J. L. 1966, Ap. J., 144, 496.

Iriarte, B. 1959, Lowell Obs. Bull., 4, 130.

Johnson, H. L., and Sandage, A. 1955, Ap. J., 121, 616.

Kowal, C. T., unpublished.

Landolt, A. U. 1973, A. J., 78, 959.

Penston, M. J. 1973, M.N.R.A.S., 164, 141.

Penston, M. J., Penston, M. V., and Sandage, A. 1971, P.A.S.P., 83, 783.

Purgathofer, A. T. 1969, Lowell Obs. Bull., 7, 98.

Sandage, A. 1970, Ap. J., 162, 841.

Sandage, A., and Kowal, C. T., unpublished.

Wing, R. F. 1973, A. J., 78, 684.

FIGURE CAPTIONS

Figure 1. A schematic representation of image digitization and processing. An idealized stellar image is shown as a distribution of photographic density over position on the film. The sampling raster pattern will define a series of "slices", such as a, b, and c. The data are written onto magnetic tape as a series of x-positions and density values, as indicated by the weighted delta functions. As each new line is read into the computer, the image slice is reduced to a single value of x-centroid and total density, then combined with the previously consolidated image. For example, the point representing line c would be combined with the single point denoting the total density and weighted centroid of lines a and b.

Figure 2. A sample film area with computer-generated overlay. The transparent overlay marks the position of the 79th ultraviolet excess object on the film. The U image is $\sim$ 25" to the right of the B image.

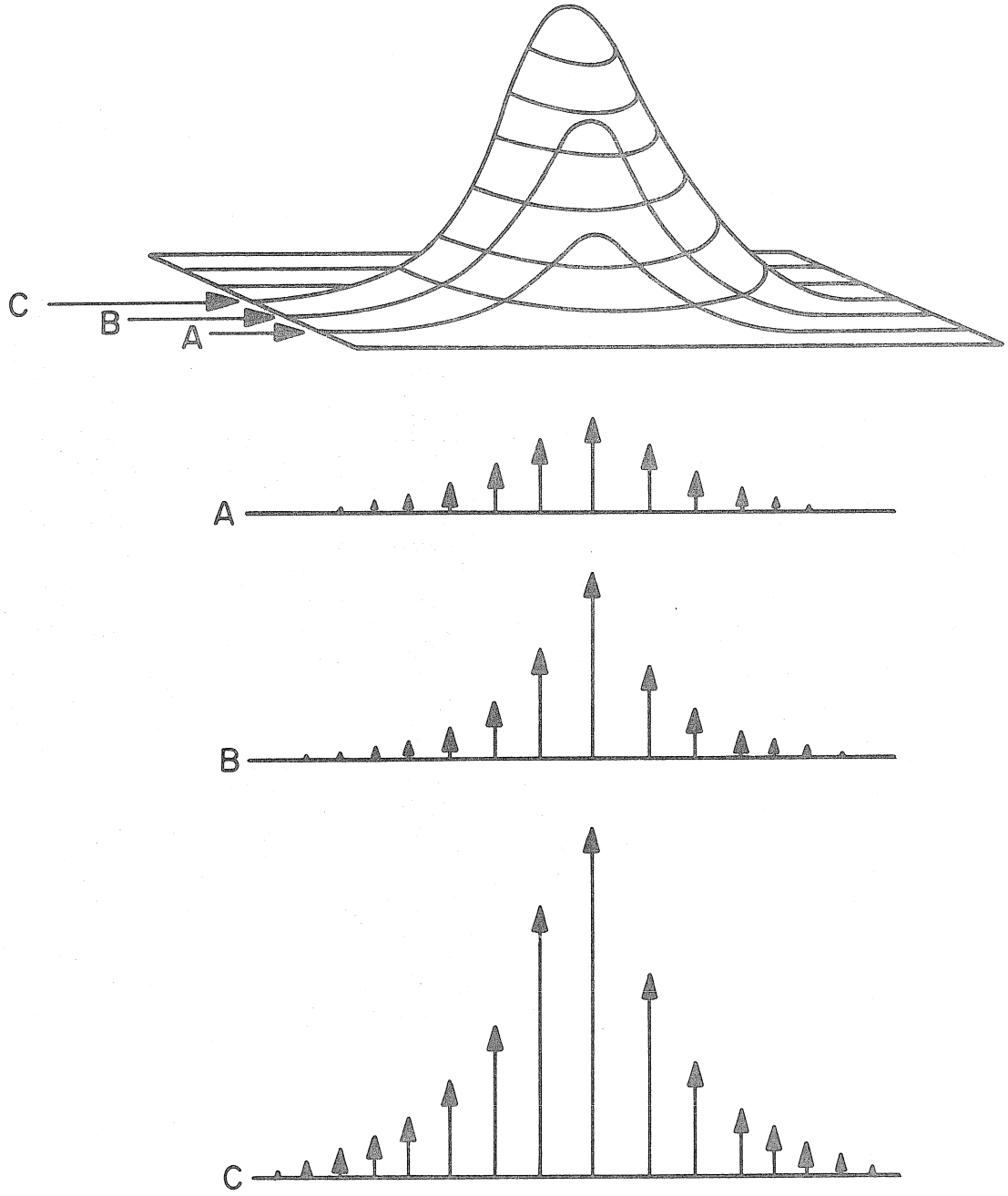

Figure 1

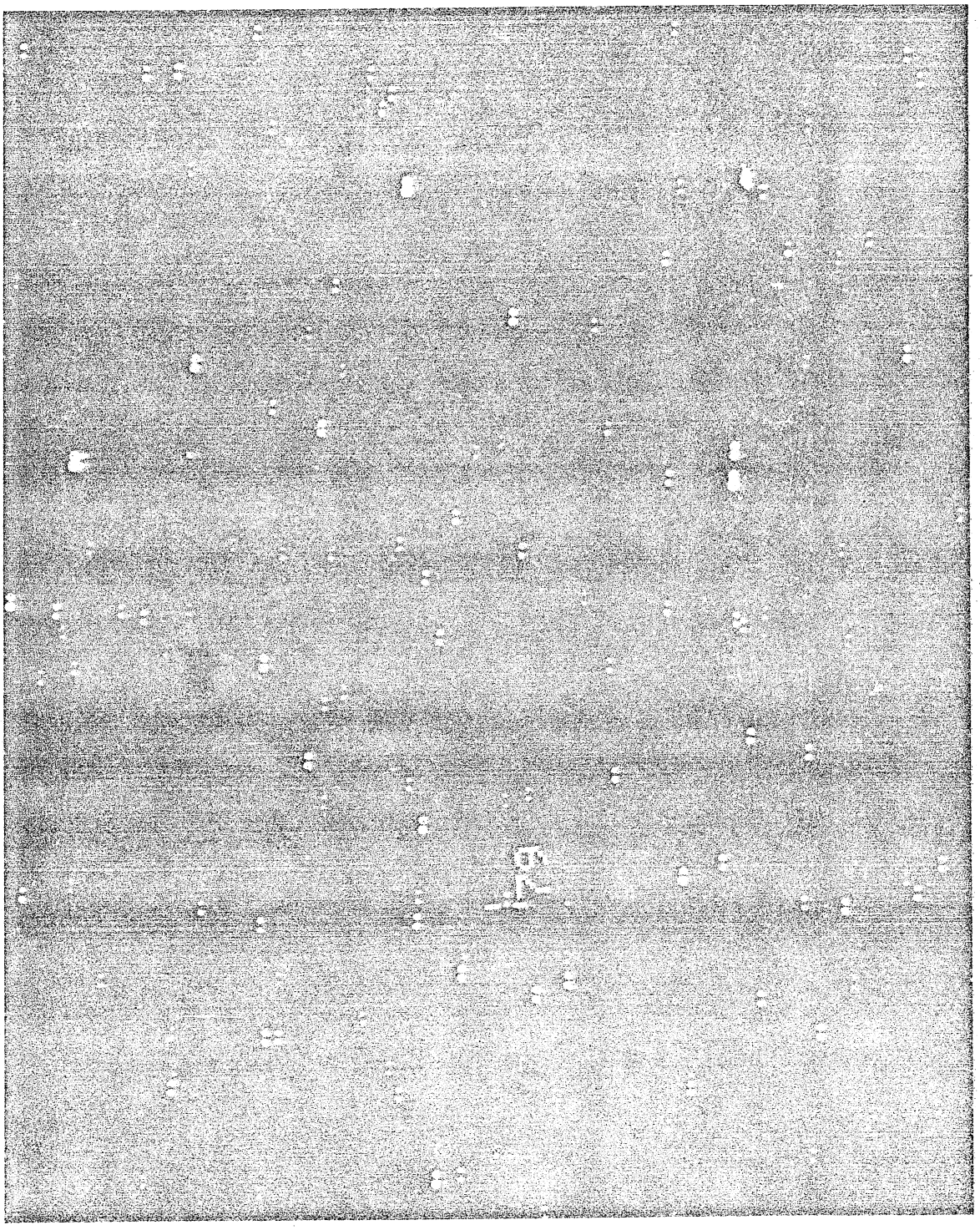

Figure 2